Two-Layer Video Codec Design for ATM Networks

Shang-Pin Chang and Hsueh-Ming Hang

Dept. of Electronics Engineering
National Chiao Tung University
Hsinchu, Taiwan 30050, ROC

Abstract

The asynchronous-transfer-mode (ATM) transmission has been adopted by most computer networks and the broadband integrated-services digital network (ISDN). Many researches have been conducted to investigate the transmission of video services over ATM networks. The previous studies often concentrate on designing video coders or on designing network regulating policies that reduce packet loss effect. But our ultimate goal should be reducing the overall distortion on the reconstructed images at the receiver and this distortion contains two components: (1) source coding error due to compression and (2) channel error due to network packet loss. In general, a high output rate at a source encoder leads to a smaller compression error; however, this high bit rate may also increase lost packets and thus increase the channel error. In this paper, a popular two-layer coding structure is considered and the optimal quantizer step size for the enhancement layer has been studied under the consideration of the source-plus-channel distortion. Through both theoretical analysis and image simulation, we indeed find an optimal operating point that achieves the lowest total mean squared error (MSE) at the receiver.

Keyword: two-layer codec, packet loss, source-plus-channel distortion

1 Introduction

Since the International Telegraph and Telephone Consultative Committee (CCITT) agreed to develop the broadband ISDN on the basis of the ATM principle, a lot of research efforts have been spent on evaluating the consequences of video services, which are to provide an important part of future data traffic. Many proposals have suggested various ways in reducing the picture distortion due to packet loss. On the other hand, the goal of source coding is to reduce the distortion due to compression. However, conventionally, these two research directions are independently studied. The ultimate image distortion at the receiver is a combination of both source coding errors and channel loss errors. To maximize the image quality at the receiver, we should consider both at the same time.

A high output rate at an encoder is likely to cause the network congested so that the reconstructed pictures are impaired because of a high cell loss rate. On the other hand, an encoder with a low output rate is less likely to bring about congestion, but the quality of reconstructed pictures are still poor due to the degradation caused by large quantizer step sizes used in source coding. In this paper, we will discuss how to determine the optimal quantizer

0-8194-1638-X/94/$6.00

step size of the enhancement layer of a two-layer codec for optimizing the reconstructed picture quality considering both source and channel losses.

The block diagram of a conventional two-layer encoder is shown in in Figure 1. The original images are first lowpassed and decimated; then, their sizes are scaled down by subsampling. These subsampled images are the inputs to the base layer — an modified RM8 (Reference Model 8) video coder (an H.261 encoder [1]), of which the bit rate regulator is removed and therefore the output rate is allowed to fluctuate — The output codes of this base layer are assigned higher priority. Decoding these codes, the low-resolution (subsampled) images can be reconstructed and then upsampled to the original resolution. Since these original-resolution pictures are linearly interpolated from the subsampled and compressed images, they are called the *interpolated pictures.* At enhancement layer, a modified JPEG image coder [2] is used to encode the residual images generated by subtracting the interpolated pictures from the originals. The output codes are the enhancement layer data. The choice of RM8 and JPEG is simply because they are well-known international standard coders. In the following simulations, the original resolution is CIF picture (*352 pels*$\times$*288 lines*), and the subsampled pictures (base-layer) are in QCIF (*176 pels*$\times$*144 lines*).

2 Total MSE Minimization

The rate-distortion (R-D) graph is typically used to illustrate the performance of a source coding algorithm. It often does not include the degradation due to channel errors such as cell loss in ATM networks. We suggest a modified R-D graph that includes both source errors and channel errors as shown in Figure 2. The solid line and the dash line represent the operating curves of a single-layer coder and of a two-layer coder, respectively. As mentioned earlier, a single-layer coder (solid line) has a high distortion at very high bit rates due to network congestion. It has also a high distortion at very low bit rates due to compression errors. Hence, it achieves the lowest distortion operating point some where in between. [3] In contract, the degradation of a two-layer coder usually will not go below a certain quality assurance, MSE_{base}. This is because the packets produced by base layer are always guaranteed to reach the receivers without loss.

One may note that the dash line in Figure 2 has a discontinuity at the distortion equaling to MSE_{base}. The lower section of the dash curve (which coincides with the solid curve) represents the R-D relation of the base-layer encoder. When the bits are lower than the lossless rate bound, no packet loss is assumed. Hence, all the bits are assigned to the base layer which is identical to a single-layer coder. However, only a certain number of bits (lossless channel rate) can be considered error free. The bit rate higher than the lossless rate is given to the enhancement layer, represented by the upper section of the dash curve. When the enhancement bit rate is low, the total distortion at the destination is mainly due to source coding. Hence, this distortion is reduced when the bit rate gets higher. However, the channel loss becomes the dominating factor of the total distortion when bits are getting too high. In between, there is an optimal operating point at which a two-layer codec reaches its best picture quality.

Thus, it shows in Figure 2 that either a single-layer or a two-layer coding algorithm exhibits a unique minimum MSE operating point. The analysis of the single-layer coding is difficult to proceed at this point since the coder

exploits temporal correlation of pictures for compression. Experimental results of an optimal single-layer video coder is reported by [3]. The analysis of a two-layer coder is easier because the enhancement-layer images are intra-coded. Image degradation caused by the losses of enhancement-layer packets do not propagate in time to the following reconstructed pictures.

Therefore, the mean-squared error between the original image and the reconstructed image for a two-layer algorithm can be computed by [4]

$$MSE_{total} = \Delta_2 MSE_{base} + (1 - \Delta_2) MSE_{enh}, \tag{1}$$

where MSE_{base} and MSE_{enh} are the source coding errors of the base-layer image and the base-plus-enhancement image, respectively, and Δ_2 represents the fraction of enhancement-layer cell loss. In other words, for the portion where enhancement packets are lost, the MSE_{total} comes from the the base-layer MSE. For the portion where the enhancement packets are received, the MSE_{total} equals to the enhancement-layer MSE.

The above equation shows that the MSE_{total} is dominated by the MSE_{base} for a high loss rate of enhancement packets, $\Delta_2 \rightarrow 1$; while at a low loss rate, $\Delta_2 \rightarrow 0$, the MSE_{enh} dominates the MSE_{total}. Although allowing a high bit rate for the enhancement layer achieves a lower MSE_{enh} and hence, a lower MSE_{total}, Δ_2 also increases due to the network congestion. This in term reduces the effectiveness of MSE_{enh} reduction. Consequently, the trade-off of MSE_{enh} and Δ_2 results in an minimal MSE_{total} operating point. The explicit expression of this operating point depends on the underline structure of the chosen two-layer codec. When the bit rate and the distortion are mainly controlled by the enhancement-layer quantizer step size (Q_2) in a typical two-layer coder described in section 1, an optimal Q_2, therefore, exists. In a two-layer codec, the MSE_{base} can be calculated at the encoder side and is independent of channel. The derivation of MSE_{enh} and Δ_2 will be shown in following two sections.

3 Bits and Distortion due to Quantization

In a two-layer coder with guaranteed base-layer data, the quality of the reconstructed complete picture is decided by the quantizer step size used by the enhancement layer, Q_2. The value of Q_2 also determines the output bits of the enhancement layer. The produced bits, in term, affect the packet loss probability of the network. Since packets of the enhancement layer may get lost in transmission, image degradation due to channel errors varies with different levels of cell loss probabilities. Therefore, the total distortion of a received picture is a combination of both source quantization and channel loss errors and both are controlled by the Q_2.

To determine an optimal Q_2 that minimizes the combined distortion due to the above two types of errors, we need to find the relationship between the source coding error and Q_2 and the relationship between the packet loss probability and Q_2. However, the above two relationships are picture-dependent. This is mainly due to the interpolation errors between the base-layer coded images and the original images. For images with smooth contents, the linear interpolation well predicts the untransmitted pixels and thus the enhancement layer produces few bits. On the other hand, for images with very active content such as textures and interlaced pictures, interpolation does

not work well and consequently the residual images generate a large number of bits.

As reported in the literature [5], a residual image values have *Truncated Discrete Laplacian* (TDL) distribution. In fact, according to our simulations, their DCT coefficients also have approximately the same type of distribution. Under this assumption, we can obtain the following two formulas representing the total entropy, H, and the mean squared error, D, of the enhancement-layer coded images as functions of Q_2 [5].

$$\begin{aligned} H(Q_2) &= \sum_{m=-N'}^{N'} -P(m)\cdot \ln P(m) \\ &= \frac{\kappa_1^2\beta_1 Q_2}{1-e^{-\kappa_1 Q_2}}\left(\beta_2 - e^{-\kappa_1(N'+\frac{1}{2})Q_2}\right) - \beta_0 \ln \beta_0 - \kappa_1\beta_1\beta_2\left(\ln\frac{\kappa_1\beta_1}{2} + \frac{\kappa_1 Q_2}{2}\right), \\ \text{and} \quad D(Q_2) &= 2\cdot\sum_{m=1}^{8Q_2} m^2\cdot P(m) \\ &= \frac{\kappa_2\left(e^{-\kappa_2}+e^{-2\kappa_2}-2e^{-\kappa_2(8Q_2+1)}\right)}{\left(1-e^{-\kappa_2}\right)^2} - \frac{\kappa_2 e^{-\kappa_2(8Q_2+1)}}{1-e^{-\kappa_2}}\cdot\left((8Q_2+1)^2-2-64e^{-\kappa_2}Q_2^2\right), \end{aligned}$$

where κ_1 and κ_2 are the parameters of the two estimated TDL distributions of the residual image values and the inversely transformed quantization errors respectively, and

$$\beta_0 = \kappa_1\left(\frac{1}{2} + \frac{e^{-\kappa_1} - e^{-\kappa_1\frac{Q_2}{2}}}{1-e^{-\kappa_1}}\right), \qquad \beta_1 = \frac{1-e^{-\kappa_1 Q_2}}{1-e^{-\kappa_1}}, \qquad \beta_2 = \frac{e^{-\kappa_1\frac{Q_2}{2}}\left(1-e^{-\kappa_1 Q_2 N'}\right)}{1-e^{-\kappa_1 Q_2}}, \tag{2}$$

$$N' = \frac{1}{\kappa_1 Q_2}\ln\frac{1}{e^{\kappa_1\frac{Q_2}{2}}\left(e^{-\kappa_1} - \left(\frac{1}{\kappa_1}-\frac{1}{2}\right)(e^{\kappa_1}-1)\right)}. \tag{3}$$

From simulation, for typical probability distribution parameters, $\frac{d(H^{-1})}{dQ_2}$ and $\frac{dD}{dQ_2}$ are nearly constant within the useful range of Q_2. Therefore, we may approximate $D(Q_2)$ and $H^{-1}(Q_2)$ by straight lines. In other words, with some bias, D is directly proportional to Q_2 while H is inversely proportional to Q_2. That is,

$$H = Bits(Q_2) = \frac{C_1}{Q_2 + C_2}, \tag{4}$$

$$\text{and} \qquad D = MSE(Q_2) = C_3 Q_2 + C_4, \tag{5}$$

where C_1, C_2, C_3, and C_4 are constants tuned to every coded picture.

For a given to-be-coded residual image, parameters (C_1, C_2, C_3, C_4) can be calculated from the data obtained by encoding the residual image using two different values of Q_2. The estimated curves (models) and the simulated curves are shown in Figure 3 for the residual image sequence of "*Footbal*l". The estimated curve is obtained by using equation (4) and (5) evaluated at $Q_2 = 10$ and $Q_2 = 26$.

4 Packet Loss Probability

Figure 4 shows our model of a packet multiplexing system. Base on this model, we derive the relationship between the packet loss probability and the multiplexor load for a general packet network. We assume the packet loss is

entirely due to the excessive delay caused by traffic congestion. That is, the channel noise is negligible. This model consists of a multiplexor and N queues served as prebuffers of the N sources. Packets in prebuffer G_i can only wait for a given time constraint K_i; otherwise, they are discarded. Therefore, the packet loss rate is $\lambda_i \pi(K_i)$ and the delivered packet rate is $\lambda_i(1-\pi(K_i))$ at prebuffer G_i. Here, $\pi(K_i)$ denotes the loss probability of G_i as a function of K_i and λ_i represents the incoming rate of G_i. We assume that the service time of the multiplexor is an exponentially distributed random variable with mean μ^{-1} *sec/packet*, i.e., a mean service rate of μ *packet/sec*. The service policy is *FCFS* (First Come First Serve) for the packets departing from all the prebuffers. As shown in [6], a smoothed video traffic can be treated as a Poisson process on a frame by frame basis. Thus we assume the packet arrival at prebuffer G_i can be modeled as a Poisson process with mean packet rate λ_i. Since we are only interested in deriving the probability of packet loss of each prebuffer without load sharing, the discarded packets are not allowed to reenter the other queues, and the derivation in [7] can be simplified.

Let $F(w,t)$ represent the probability of that the remaining packets in a prebuffer at time t is less than or equal to w. If $B(x)$ denotes the accumulated probability density function of the service time distribution at the multiplexor, the time-evolution equation of $F(w,t)$ can be described as bellow. To simplify the notations in the following equations, the time unit is taken as *second/packet*. Hence, $(\lambda_i \Delta t)$ represents the received packet number per packet time duration.

$$F(w,t+\Delta t) = \prod_{i=1}^{N}(1-\lambda_i \Delta t)F(w+\Delta t,t) + \sum_{j=1}^{N}\prod_{i=1,i\neq j}^{N}\lambda_j \Delta t(1-\lambda_i \Delta t)\int_0^w B(w-u)d_u F(u,t), \tag{6}$$

where $F(w,t+\Delta t)$ is the probability that the remaining packets in a prebuffer at time $t+\Delta t$ is less than w. The first term on the right-hand side represents the case that no packets may arrive in the time interval $[t,t+\Delta t]$ and the number of packets in the buffer are less than $w+\Delta t$ at time t. The second term indicates the sum of probabilities that each of them represents the case that exactly one packet arrives during time interval Δt and the total undelivered packets at $t+\Delta t$ is less than w.

Rearranging the terms in (6) and taking limits as $\Delta t \to 0$, we obtain

$$\frac{\partial F(w,t)}{\partial t} - \frac{\partial F(w,t)}{\partial w} = \sum_{i=1}^{N}\lambda_i \left\{\int_0^w B(w-u)d_u F(u,t) - F(w,t)\right\}. \tag{7}$$

As shown in [6], the system will quickly reach steady state compared to the duration of the frame time. Thus, by taking limits as $t \to \infty$, we obtain the following steady-state equation,

$$\frac{dF(w)}{dw} = \sum_{i=1}^{N}\lambda_i \left\{F(w) - \int_0^w B(w-u)d_u F(u)\right\}. \tag{8}$$

In the case that the multiplexor service time is exponentially distributed with a mean of μ^{-1}, the solution to (8) is given by

$$F(w) = F(0^+)\left\{\frac{\mu}{\mu-\sum\lambda_i} - \frac{\sum\lambda_i}{\mu-\sum\lambda_i}e^{-w(\mu-\sum\lambda_i)}\right\}. \tag{9}$$

Since we are only interested in computing the fraction of packet loss, we introduce the concept of flow conservation to derive the second equation as follows.

$$\sum_{i=1}^{N} \lambda_i = \{1 - F(0^+)\}\mu + \sum_{i=1}^{N} \{1 - F(K_i)\}\lambda_i \tag{10}$$

The left-hand side of the above equation represents the total packet flow into the N prebuffers. The first term on the other side represents the departure packet stream from the multiplexor, and the second indicates the total lost packet flow in the N prebuffers due to congestion.

Assuming that we now consider a single video coder producing time-constrained packets and the other $N-1$ sources sending time-senseless packets, we can then treat the packets sent by those $N-1$ sources as lossless packets. This assumption can be realized as one queue with a short time constraint and the others with very loose constraints. That is, the lossless fraction $F(K_{long})$ of the time-senseless queue with a long time constraint approaches 1. Then (10) can be simplified as shown below.

$$\sum_{i=1}^{N} \lambda_i = \{1 - F(0^+)\}\mu + \{1 - F(K_1)\}\lambda_1, \tag{11}$$

where K_1 refers to the short time constraint and λ_1 represents the outgoing rate of *Source* 1 (the video source), which producing time-sensitive packets. Note that we have assumed that *Source* 1 is a video encoder whose output packets have a much larger variation than the packets from the other normal variable-bit-rate sources. This is, in fact, approximately true even when the other sources are video sources with a fixed image quality. In this case, the total flow rate of the other sources except *Source* 1 can be regarded as a constant bit rate flow [8]. We denote the total flow rate of the $N-1$ VBR sources as λ_0 and rewrite (9) and (11) to

$$F(w) = F(0^+)\left\{\frac{\mu}{\mu - \lambda_0 - \lambda_1} - \frac{\lambda_0 + \lambda_1}{\mu - \lambda_0 - \lambda_1} e^{-w(\mu - \lambda_0 - \lambda 1)}\right\}, \tag{12}$$

and

$$\lambda_0 + \lambda_1 = \{1 - F(0^+)\}\mu + \{1 - F(K_1)\}\lambda_1. \tag{13}$$

Since K_1, μ, and λ_0 can now be viewed as constants, we can solve the above two simultaneous equations to obtain the loss probability of *Source* 1, $\pi(\lambda_1)$, as a function of λ_1,

$$\pi(\lambda_1) = \frac{(\mu - \lambda_0 - \lambda_1)(\lambda_0 + \lambda_1)e^{-K_1(\mu - \lambda_0 - \lambda_1)}}{\mu(\mu - \lambda_0 - \lambda_1) + \lambda_1(\mu - (\lambda_0 + \lambda_1))e^{-K_1(\mu - \lambda_0 - \lambda_1)}}. \tag{14}$$

By definition, $\pi(\lambda_1)$ is $1 - F(K_1)$. Figure 5 shows its curves under different background loads, λ_0. From these curves, $\pi(\lambda_1)$ can thus be approximated by a quadratic function,

$$\pi(\lambda_1) = \alpha_2 \lambda_1^2 + \alpha_1 \lambda_1 + \pi_0, \tag{15}$$

where α_1, α_2 and π_0 are parameters determined by the *delay constraint, mean service time,* and the *current network load.*

5 Final Results

By combining the set of equations, (4), (5), and (15), under the following converting formula,

$$Packet\ arrival\ rate = \lambda = frame\ rate\ \frac{frame\ bits}{cell\ payload\ size}, \tag{16}$$

equation (1) can be restated as below,

$$MSE_{total}(Q_2) = MSE_{enh}(Q_2) + \pi_{enh}(Q_2)\,(MSE_{base} - MSE_{enh}(Q_2)). \tag{17}$$

After replacing every Q_2 functions by its approximate expression, we have

$$MSE_{total}(Q_2) = C_3Q_2 + C_4 + \left(\alpha_2\left(\frac{C_1 f}{R}\frac{1}{Q_2+C_2}\right)^2 + \alpha_1\left(\frac{C_1 f}{R}\frac{1}{Q_2+C_2}\right) + \pi_0\right) \cdot (MSE_{base} - C_3Q_2 - C_4),$$

where f denotes the *frame rate* and R represents the *cell payload size*.

Denoting MSE_{base} as E_b, MSE_{total} as E_t, and $Q_2 + C_2$ as Q_{bias}, we have

$$\begin{aligned}
E_t(Q_{bias}) &= \frac{1}{Q_{bias}^2}\left\{Q_{bias}^2\,(C_3(Q_{bias}-C_2)+C_4) + Q_{bias}^2\pi_0\,(E_b - C_3(Q_2-C_2)-C_4)\right. \\
&\quad +\alpha_2\left(\frac{C_1 f}{R}\right)(E_b - C_3(Q_{bias}-C_2)-C_4) \\
&\quad \left.+Q_{bias}\alpha_1\left(\frac{C_1 f}{R}\right)(E_b - C_3(Q_{bias}-C_2)-C_4)\right\} \\
&= \frac{1}{Q_{bias}^2}\left\{(C_3 - C_3\pi_0)Q_{bias}^3 + \left(-C_2C_3 + C_4 + C_2C_3\pi_0 - C_4\pi_0 + E_b\pi_0\right.\right. \\
&\quad \left.-\alpha_1 C_3\left(\frac{C_1 f}{R}\right)\right)Q_{bias}^2 + \left(-\alpha_2 C_3\left(\frac{C_1 f}{R}\right) + \alpha_1\left(\frac{C_1 f}{R}\right)(E_b + C_2C_3 - C_4)\right) \\
&\quad \left.\cdot Q_{bias} + \alpha_2\left(\frac{C_1 f}{R}\right)(E_b + C_2C_3 - C_4)\right\} \\
&= \frac{1}{Q_{bias}^2}\left\{\omega_3 Q_{bias}^3 + \omega_2 Q_{bias}^2 + \omega_1 Q_{bias} + \omega_0\right\}.
\end{aligned}$$

Setting the first derivative of $E_t(Q_{bias})$ (with respect to Q_{bias}) to be zero, we can obtain

$$\begin{aligned}
&\frac{d}{dQ_{bias}}\left\{\frac{1}{Q_{bias}^2}\left\{\omega_3 Q_{bias}^3 + \omega_2 Q_{bias}^2 + \omega_1 Q_{bias} + \omega_0\right\}\right\} = 0 \\
\Rightarrow\ &\frac{1}{Q_{bias}^3}\left\{\omega_3 Q_{bias}^3 - \omega_1 Q_{bias} - 2\omega_0\right\} = 0 \\
\Rightarrow\ &Q_{bias}^3 - \frac{\omega_1}{\omega_3}Q_{bias} - 2\frac{\omega_0}{\omega_3} = 0 \\
\Rightarrow\ &Q_{bias}^3 + \Omega_1 Q_{bias} + \Omega_0 = 0
\end{aligned} \tag{18}$$

The unique positive real root of (18) is thus given as [5]

$$Q_{bias} = \frac{\Omega}{3} - \frac{\Omega_1}{\Omega}, \quad \text{where } \Omega = \sqrt[3]{\frac{-27\Omega_0 + \sqrt{108\Omega_1^3 + 729\Omega_0^2}}{2}}. \tag{19}$$

Note that Q_{bias} represents $Q_2 + C_2$. Therefore, the optimal quantizer step size is $Q_{bias} - C_2$.

Figure 6 shows the MSE_{total} curve of a simulation result (the solid line) and the corresponding curve derived from approximation formula (the dash line). It can be observed that the optimal Q_2 we estimated is quite close to the actual one.

6 Conclusions

In summary, we first point out that there should exist an optimal operating point on the rate-distortion curve for a variable-bit-rate two-layer video coder operated in the finite bandwidth ATM environment. For a popular two-layer codec using standard compression algorithms, such an operating point can be explicitly expressed in terms of quantizer step size selection. In order to compute this optimal point, we demand proper channel model and source model. Based on a general multiplexing model, we derive an approximate expression of packet loss probability that serves as the channel model. And two approximations are derived to represent the entropy and the distortion aspects of the source model. Then on the basis of these models, an optimal enhancement-layer quantizer step size is obtained by considering both source quantization distortion and channel loss error. Simulations on real pictures verify the existence of the optimal operating point and demonstrate that our approximation is very close to the actual one.

References

[1] "Description of Reference Model (RM8)," Document 525, CCITT Study Group XV, Working Party XV/4, Specialist Group on Coding for Visual Telephony, June 9, 1989.

[2] W. B. Pennebaker and J. L. Mitxhell, "JPEG - still image data compression standard," New York: Van Nostrand Reinhold, 1993.

[3] T. Y. Mei and H. M. Hang, "On Optimal Video Codec Design for ATM Networks with Finite Bandwidth," PCS'94, Davis, CA, U.S.A, September, 1994.

[4] S. P. Morgan and A. R. Reibman, "Statistical Multiplexing Comparison of One- and Two-layer Video Codec for Teleconferencing," June 1992.

[5] S. P. Chang, "Two-Layer Video Codec Design for Packet Networks," M.S. Thesis, Institute of Electronics, National Chiao Tung University, Taiwan, R.O.C., June 1994.

[6] P. Skelly, S. Dixit, and M. Schwartz, "A Histogram-Based Model for Video Traffic Behavior in a ATM Network Node with an Application to Congestion Control," IEEE INFOCOM'92, pp. 95-104, 1992.

[7] J. F. Kurose and R. Chipalkatti, "Load Sharing in Soft Real-Time Distributed Computer Systems," IEEE Trans. on Computers, Vol. C-36, No. 8, pp. 993-1000, August 1987.

[8] B. G. Haskell, "Buffer and Channel Sharing by Several Interframe Picturephone Coders," Bell System Tech. Journal, Vol. 51, No. 1, pp. 261-298, January 1972.

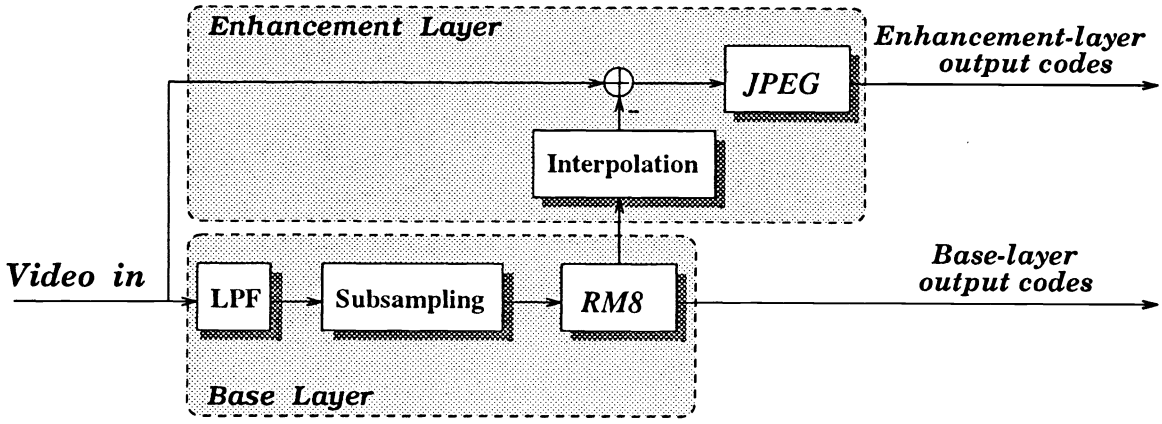

Figure 1: Functional block diagram of a general two-layer encoder

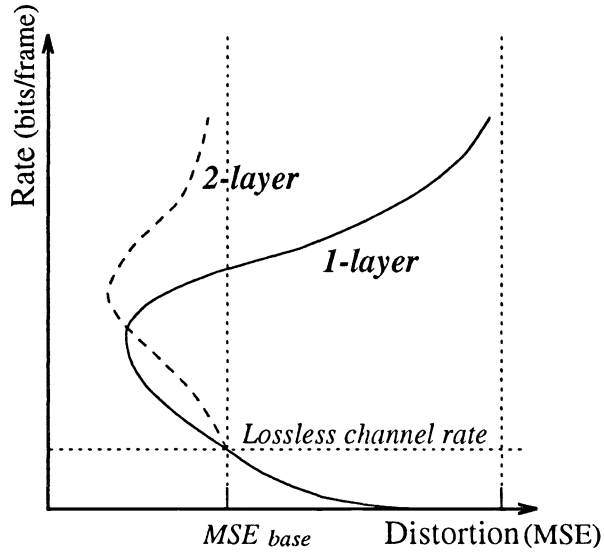

Figure 2: Rate-Distortion chart of single-layer and two-layer codecs considering both source and channel losses.

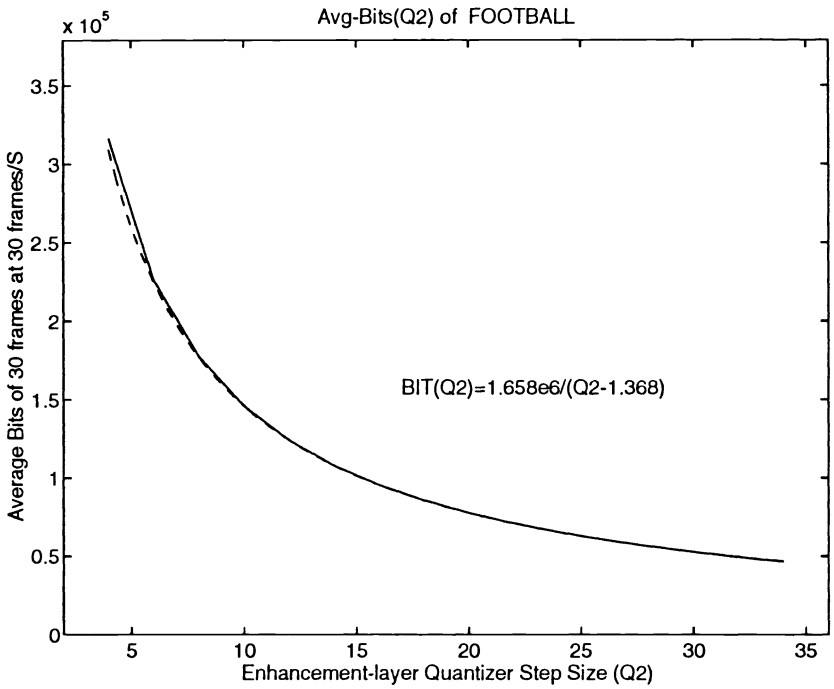

(a)

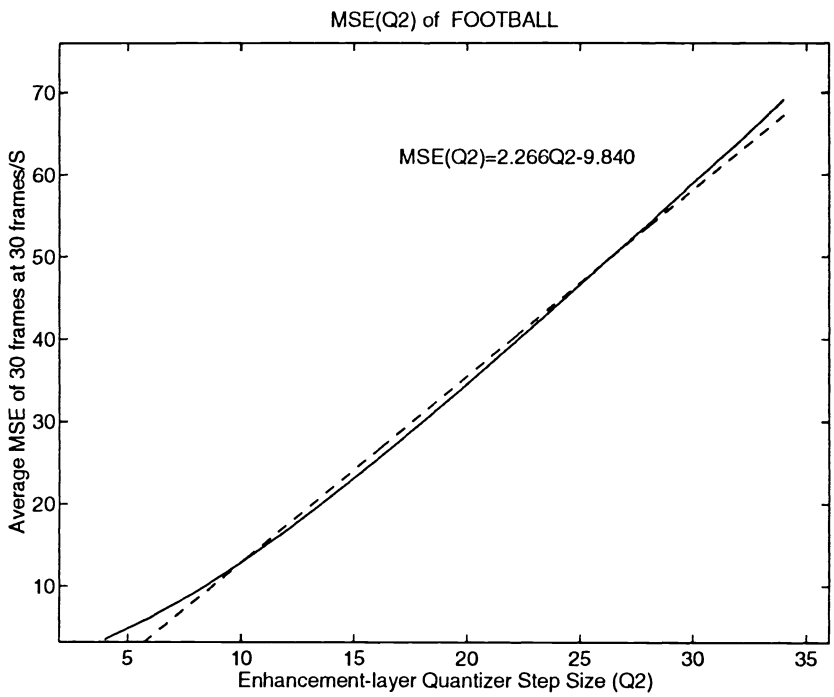

(b)

Figure 3: (a) Simulated $Bits(Q_2)$ curve and the approximate curve (2) and (b) Simulated $MSE(Q_2)$ curve and the approximate curve (3) for the "*Football*" sequence.

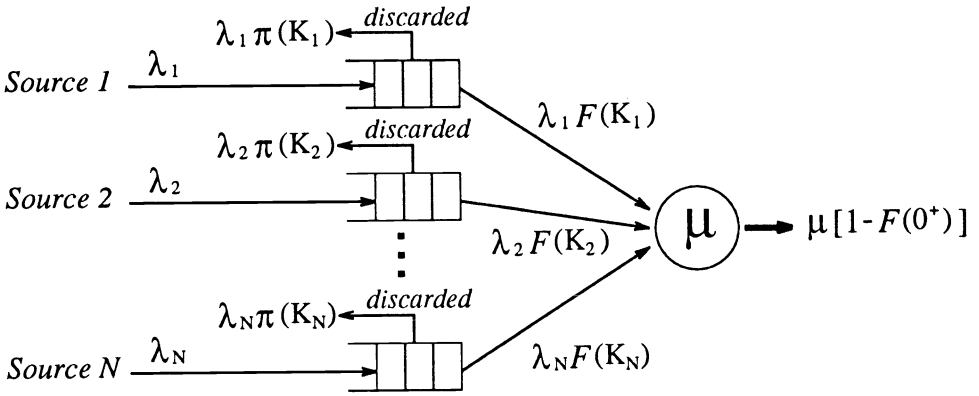

Figure 4: A Multiplexing model for deriving cell loss probability

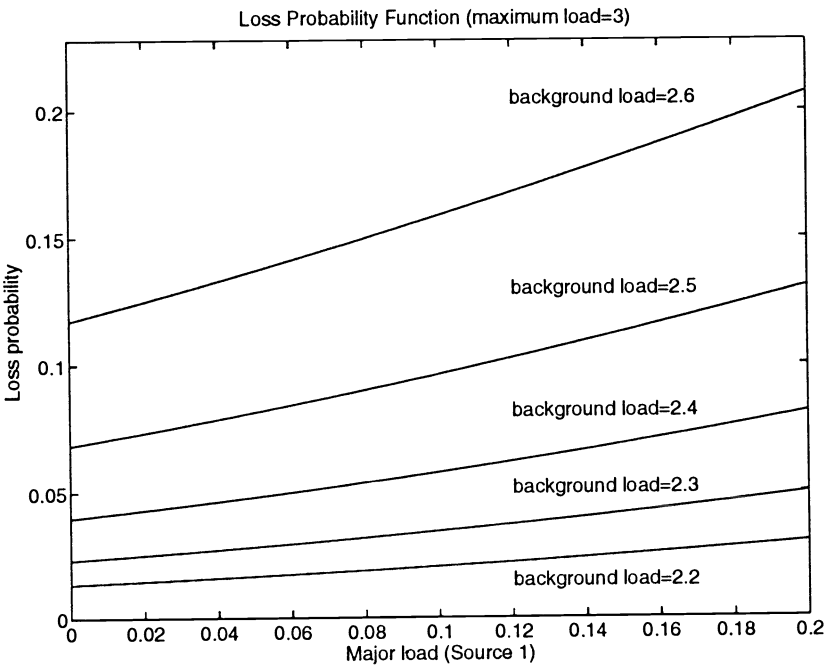

Figure 5: Loss probability function with different background loads

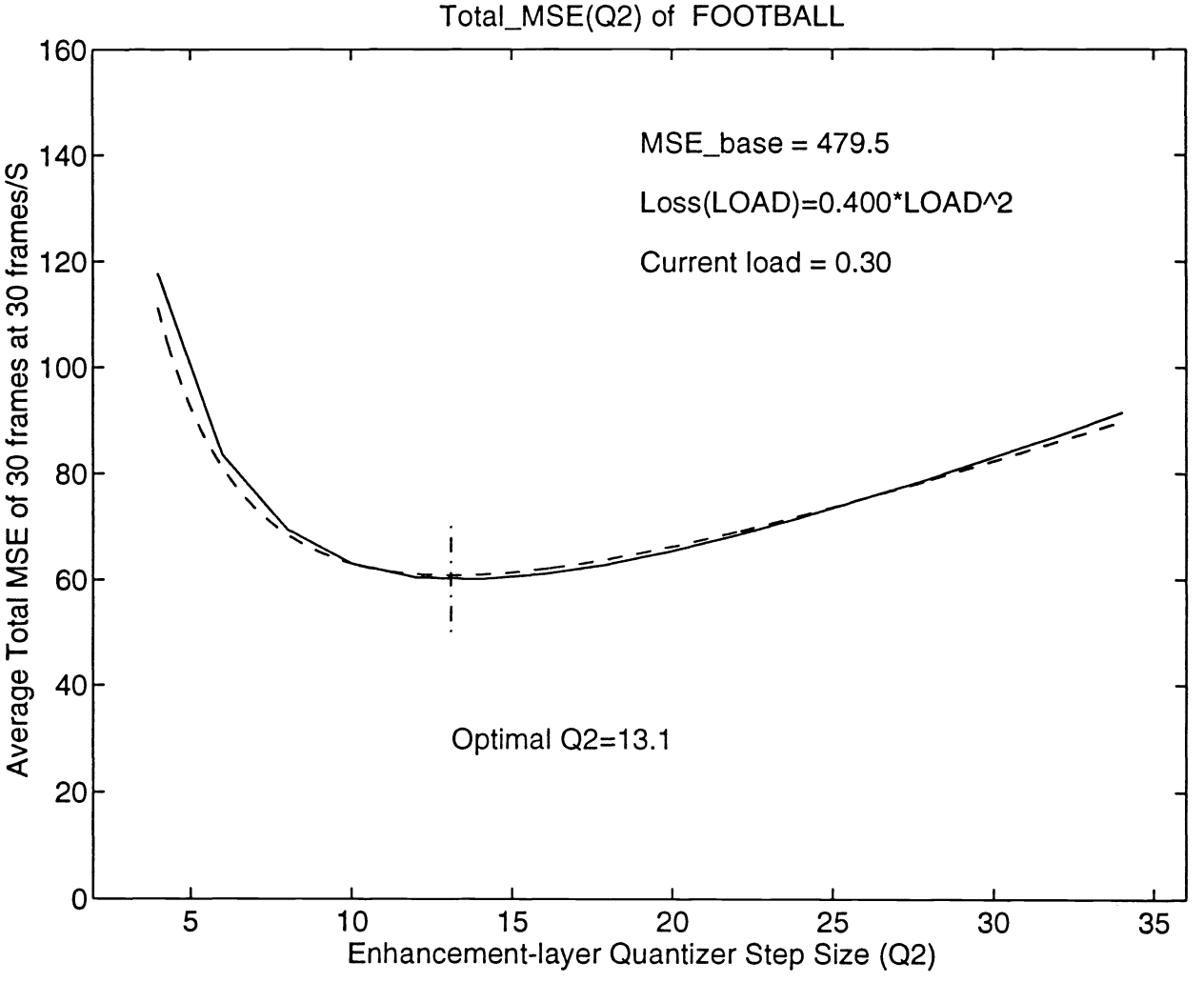

Figure 6: Total MSE curve (solid line for the simulated and dash line for the approximated results)